nature publishing group

Influenza A facilitates sensitization to house dust mite in infant mice leading to an asthma phenotype in adulthood

A Al-Garawi[1], R Fattouh[1], F Botelho[1], TD Walker[1], S Goncharova[1], C-L Moore[1], M Mori[2], JS Erjefalt[2], DK Chu[1], AA Humbles[3], R Kolbeck[3], MR Stampfli[1], PM O'Byrne[4], AJ Coyle[1,3] and M Jordana[1]

The origins of allergic asthma, particularly in infancy, remain obscure. Respiratory viral infections and allergen sensitization in early life have been associated with asthma in young children. However, a causal link has not been established. We investigated whether an influenza A infection in early life alters immune responses to house dust mite (HDM) and promotes an asthmatic phenotype later in life. Neonatal (8-day-old) mice were infected with influenza virus and 7 days later, exposed to HDM for 3 weeks. Unlike adults, neonatal mice exposed to HDM exhibited negligible immune responsiveness to HDM, but not to influenza A. HDM responsiveness in adults was associated with distinct Ly6c$^+$ CD11b$^+$ inflammatory dendritic cell and CD8α^+ plasmacytoid (pDC) populations that were absent in HDM-exposed infant mice, suggesting an important role in HDM-mediated inflammation. Remarkably, HDM hyporesponsiveness was overcome when exposure occurred concurrently with an acute influenza infection; young mice now displayed robust allergen-specific immunity, allergic inflammation, and lung remodeling. Remodeling persisted into early adulthood, even after prolonged discontinuation of allergen exposure and was associated with marked impairment of lung function. Our data demonstrate that allergen exposure coincident with acute viral infection in early life subverts constitutive allergen hyporesponsiveness and imprints an asthmatic phenotype in adulthood.

INTRODUCTION

Allergic asthma (AA), the most prevalent chronic inflammatory disease during childhood,[1] is characterized by airway inflammation, variable airflow obstruction, and reduced lung function, and is associated with structural remodeling of the airways. Despite remarkable progress in our understanding of the pathogenesis of this disease, elucidation of its origins, i.e., of the conditions under which AA emerges, remains elusive. Increasingly, environmental factors are believed to have preeminent roles in the emergence of allergic diseases, including asthma. In this context, acute respiratory viral infections are a major health threat in early life, and epidemiological studies have shown that by 2 years of age, most children will have been infected with at least one respiratory virus.[2,3] Importantly, those respiratory viral infections in early life that result in wheezy lower respiratory illness are associated with persistent wheezing, asthma, and reduced lung function at 6 years of age.[4,5] In addition, allergen sensitization to perennial allergens before the age of 2 years, but not later in childhood, is associated with a decrease in lung function and the presence of allergic airway disease in school-aged children.[6–8] What remains to be established is a direct causative link between viral infections and allergen sensitization in infancy with AA in later life.

That the majority of infants who wheeze do not develop AA suggests that tolerance, a state of homeostatic responsiveness, is the natural response to innocuous aeroallergens. Therefore, the generation of an immune-inflammatory response to aeroallergens assumes that tolerance was either prevented or subverted. Speculatively, profound perturbations of the lung microenvironment, especially during development, such as those caused by viral infections may prime the local immune environment to trigger immune-inflammatory responses to otherwise innocuous allergens.

[1]Division of Respiratory Diseases and Allergy, Center for Gene Therapeutics and Department of Pathology and Molecular Medicine, McMaster University, Hamilton, Ontario, Canada. [2]Department of Experimental Medical Science, Lund University, Lund, Sweden. [3]Department of Respiratory, Inflammation and Autoimmunity, MedImmune LLC, Gaithersburg, Maryland, USA. [4]Department of Medicine, McMaster University, Hamilton, Ontario, Canada. Correspondence: M Jordana (jordanam@mcmaster.ca)

Received 19 November 2010; accepted 28 June 2011; published online 31 August 2011. doi: 10.1038/mi.2011.35

In this study, we investigated the interaction between viral infection and allergen sensitization in early life, and determined its structural and functional consequences into adulthood. We chose influenza A because the rate of influenza infection in pre-school children is estimated to be up to 40% annually with at least 1% resulting in hospitalization. Importantly, children younger than 6–12 months of age are at the highest risk of severe infection.[9] We also chose house dust mite (HDM) because it is the most pervasive common aeroallergen worldwide and permits studying mucosal immune-inflammatory responses in the absence of exogenous confounding adjuvants.

Our data show that, compared with adults, infant mice are immunologically hyporesponsive to a relatively high dose of HDM. In contrast, infant mice generate a robust immune-inflammatory response to influenza A infection. This influenza-induced environment facilitates allergen responsiveness, leading to airway inflammation, Th2 immunity, and evidence of both airway and lung parenchymal remodeling. Importantly, these structural changes persist into adulthood and are now associated with marked lung dysfunction even after a prolonged period of absence to allergen exposure and resolved inflammation.

RESULTS

HDM-mediated airway inflammation in early life

To determine the impact of aeroallergen exposure in early life, we exposed 2-week-old (infant) mice to 25 μg HDM for 3 weeks and compared the inflammatory response to an identical exposure in 8-week-old (adult) mice. Our data show, as reported previously, that adult mice responded with a robust inflammatory response including a substantial influx of eosinophils (43%) (data not shown); in sharp contrast, infant mice exhibited minimal lung inflammation, including eosinophilia (**Figure 1a–c**). In light of these data, we evaluated levels of transforming growth factor (TGF)-β1 and interleukin (IL)-10, cytokines with known anti-inflammatory and immune-regulatory properties, in the lungs of 2-, 5-week-old, and adult mice. Naive infant mice exhibited a 4–5-fold increase in the levels of active TGF-β1 over those observed in naive 5-week-old and adult mice. Similarly, IL-10 levels in naive 2-week-old mice diminished with increasing age (**Figure 1d** and **e**).

Next, we examined whether an ongoing influenza A infection altered responses to HDM. Groups of 8-day-old (neonatal) mice were either infected with influenza A virus (Flu) or given phosphate-buffered saline (PBS), and 7 days later at the peak of influenza-induced inflammation, were exposed to either HDM or saline (Sal) for 3 weeks (**Figure 2a**). Mice infected with influenza or exposed to HDM alone had only minimal inflammation at this time point, whereas mice exposed to HDM in the context of an influenza infection exhibited dramatically enhanced inflammation, similar to that observed in adult mice (**Figure 2b**). The increase in total inflammation was associated with significant increases in the numbers of mononuclear cells and eosinophils in the bronchoalveolar (BAL) and tissue (**Figure 2b** and **c**). In addition, we observed a modest 2.4-fold increase in the number of neutrophils following influenza A infection after co-exposure with HDM over that in mice infected with influenza only, but not in mice exposed to HDM alone. These local inflammatory changes were accompanied by changes in systemic immunity. Indeed, HDM-specific IgE, IgG_1, and IgG_{2a} levels were elevated only in mice exposed to HDM in the context of an influenza infection, whereas influenza-specific IgG responses were not altered by allergen exposure (**Figure 2d**).

Activation of the immune surveillance system in neonatal mice

To elucidate how influenza A infection may alter the immunoresponsiveness of neonatal mice to HDM exposure, we evaluated the impact on relevant components of the innate immune-sensing machinery. To this end, we examined the expression levels of several Toll-like receptors (TLRs) in the lungs of 8-day-old

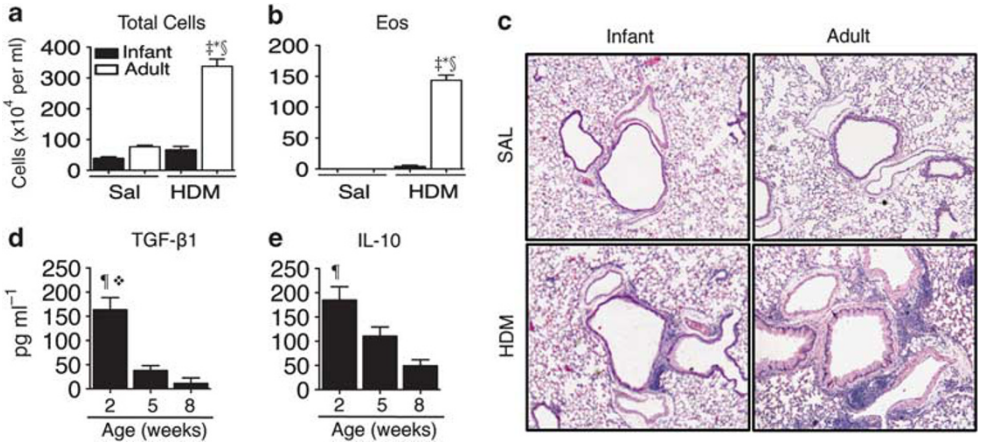

Figure 1 Impact of house dust mite (HDM) exposure in infant and adult mice. Infant and adult mice were exposed either to 3 weeks of 25 μg HDM or Sal and killed 72 h after the last HDM exposure. Cellular profile showing (**a**) total cell number and (**b**) absolute number in the bronchoalveolar lavage fluid (BAL). (**c**) Lung histopathology was evaluated by H&E to assess the degree of total lung inflammation. All images taken at ×50 total magnification as indicated. (**d**, **e**) Cytokine levels of active TGF-β and IL-10 in the lungs of naive mice at 2, 5, and 8 weeks of age. $n = 5$–8 mice per group. One of two representative experiments is shown. Data represent mean±s.e.m. $P < 0.001$ compared with *Sal (infant), ‡Sal (adult), and §HDM (infant), respectively. ■ (infant), □ (adult). $P < 0.01$ compared with ❖5 and ¶8-week-old mice. H&E, hematoxylin and eosin; IL-10, interleukin-10; TGF-β, transforming growth factor-β.

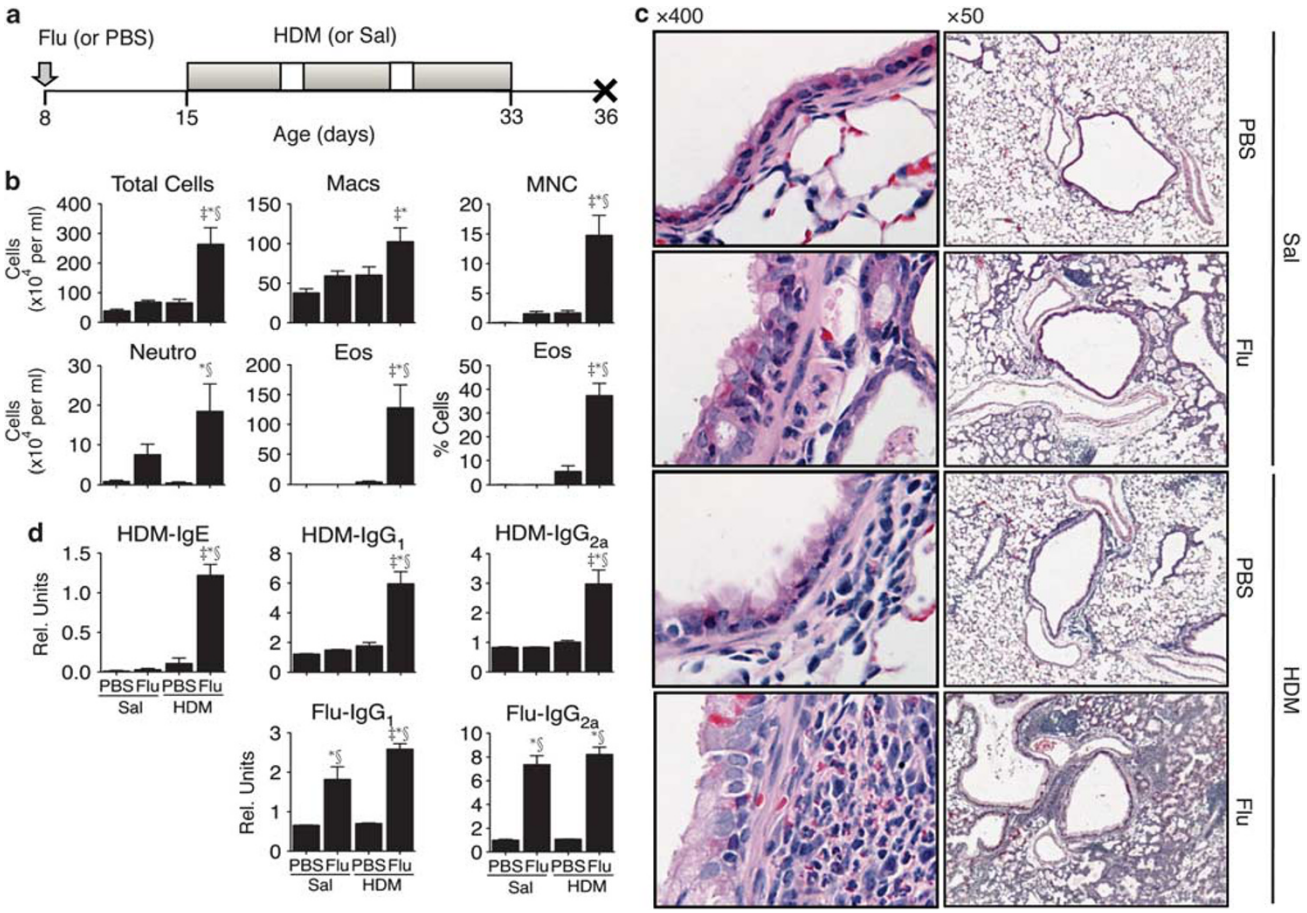

Figure 2 Impact of influenza A infection on subsequent house dust mite-induced inflammation in early life. (**a**) Eight-day-old mice were infected with influenza virus (Flu) or given PBS alone. Seven days later, PBS- and Flu-infected groups are exposed either to 3 weeks of HDM or Sal and killed 72 h after the last HDM exposure. (**b**) Cellular profile in BAL fluid showing the number of total cells, macrophages (Macs), mononuclear cells (MNC), neutrophils (Neutro), eosinophils (Eos), and the percentage of eosinophils. (**c**) Lung histopathology was evaluated by H&E to assess the degree of total lung inflammation and eosinophilia. All images taken at ×50 and ×400 total magnification as indicated. (**d**) Serum Ig levels measured by ELISA showing HDM-specific IgE, IgG1, and IgG2a and Flu-specific IgG1 and IgG2a. For all data, $n=8$–12 mice per group. One of two representative experiments is shown. Data represent mean±s.e.m. $P<0.001$ compared with *Sal, ‡Flu, and §HDM, respectively, except Flu-IgG1, $P<0.01$ compared with ‡Flu. ELISA, enzyme-linked immunosorbent assay; H&E, hematoxylin and eosin; HDM, house dust mite; PBS, phosphate-buffered saline.

mice that were either infected with influenza A or exposed to 25 μg of HDM for 7 consecutive days. Our data show that only infection with influenza A led to significantly increased levels in TLR 2, 4, 7, and 9 (**Figure 3a**).

In addition to TLR expression, we evaluated the changes in antigen-presenting cell (APC) subtypes and T cells in the lungs of 8-day-old mice either infected with influenza virus, at day 7 post infection (p.i.), or exposed to 25 μg HDM for 7 consecutive days; we used this protocol to control for changes due to age. To identify various APC subtypes, 13-color flow cytometry was used. $CD45^+/CD3^-$ cells were first gated on B220 and CD11c expression and four populations, R1–R4, selected (**Figure 3b** and **Supplementary Figure 1a** online). On the basis of this initial gating strategy, we then classified APC subtypes in the lungs of neonatal mice into distinct subsets (outlined in **Supplementary Figure 1b–d** online) and identified B cells, $Ly6C^{hi}$ monocytes, and alveolar macrophages, as previously reported in adult mice.[10–12] We also identified conventional dendritic cells (DCs) which could be further subdivided, based on CD11b and CD103 expression, into $CD11b^-(CD103^+)$ and $CD11b^+(CD103^-)$ DCs, representing intraepithelial DCs and inflammatory DCs (iDC), respectively.[13] Furthermore, within the R1 gate ($B220^+CD11c^{int}$ population), we identified a heterogeneous mixture of cells that includes NK cells and two plasmacytoids (pDCs) subtypes, $CD11b^-(CD8\alpha^-)$ and a $CD11b^-(CD8\alpha^+)$ population representing an activated pDC subset[14–16] (**Supplementary Figure 2a–c** online). Moreover, within this gate, we observed the emergence of a distinct population of $Ly6C^+$ $CD11b^+(CD8\alpha^-)$ DCs, most similar in phenotype to iDCs (iDC-like)[17,18] (**Supplementary Figure 2c** online). Neonatal mice infected with influenza virus showed a dramatic increase in NK cells and monocytes, as well as significant increases in pDCs and B cells (**Figure 3c** and **Supplementary Figure 3** online). Moreover, influenza A infection led to statistically significant increased numbers in the $B220^{hi}$ iDC-like population, but not intraepithelial DCs and conventional iDCs.

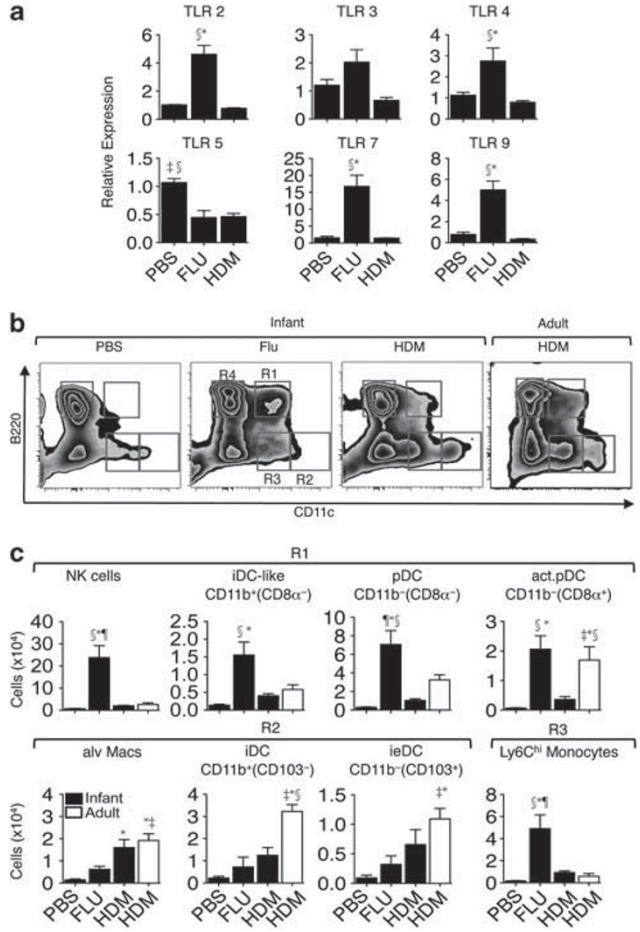

Figure 3 Lung immune status following influenza A infection or house dust mite exposure in neonatal mice. Groups of 8-day-old mice were either infected with influenza A, PBS treated, or exposed to HDM for 7 consecutive days, and adult mice exposed to HDM for 7 days. (**a**) Quantitative real-time PCR showing relative mRNA expression levels of TLR 2, 3, 4, 5, 7, and 9 in the lungs of neonatal mice infected with influenza A or exposed to HDM and compared with PBS-treated mice. $n=3$–4 mice per group. (**b**) Flow cytometric analysis of the APC compartment in whole lung digests at 7 days p.i. or 24 h after last HDM exposure using gating strategy shown in **Supplementary Figures 1** and **2** online. Representative Zebra plots showing B220 and CD11c expression and frequency of distinct immune cells populations present in the lungs of neonatal and adult mice. Gates were drawn and labeled R1–R4 as shown. (**c**) Number of NK cells, pDCs, act. pDC, and iDC-like populations, Ly6C$^+$ monocytes, alvMacs, ieDCs, and iDCs. Data representative of at least three independent experiments. $n=4$–6 mice per group. Data represent mean±s.e.m. $P<0.05$ compared with *PBS, ‡Flu, §HDM, and ¶HDM-adult, respectively. ieDC, intraepithelial DC; iDC, inflammatory DC; pDC, plasmacytoid DC; act. pDC, activated pDC; iDC-like, inflammatory DC-like; alvMacs, alveolar macrophages. ■ (infant), □ (adult). APC, antigen-presenting cell; HDM, house dust mite; PBS, phosphate-buffered saline; p.i., post infection; TLR, Toll-like receptor.

By comparison, exposure to HDM in both neonates and adult mice resulted in statistically significant increases in alveolar macrophages; however, only adult mice exhibited statistically significant increased numbers of intraepithelial DCs. Interestingly, adult, but not neonatal, HDM-exposed mice exhibited a significant increase in both iDCs and CD8α$^+$ pDCs, similar to that observed in influenza-infected neonatal mice.

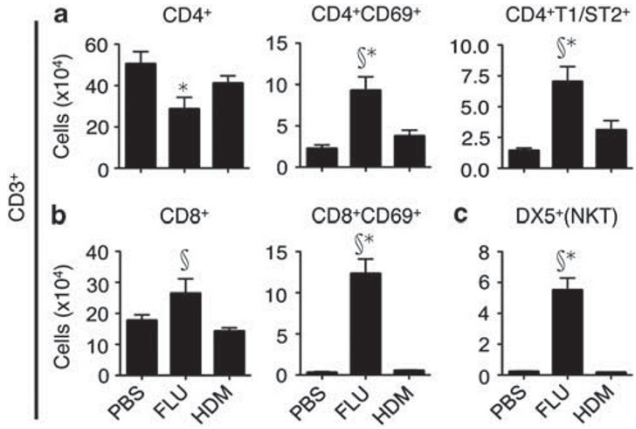

Figure 4 Impact on T-cell compartment in the lungs of neonatal mice following influenza A or house dust mite exposure. Groups of 8-day-old mice were either infected with influenza A, PBS treated, or exposed to HDM for 7 consecutive days and T cells evaluated by flow cytometry at day 7 p.i. or 24 h after last HDM exposure. (**a**, **b**) Absolute number of CD4$^+$ and CD8$^+$ T cells (CD3$^+$), their activation states (CD69$^+$), and expression of Th2 cell surface marker, T1/ST2. (**c**) Absolute number of DX5$^+$ (CD3$^+$) NK-T cells. For all data, $n=5$–6 mice per group. One of two representative experiments is shown. Data represent mean± s.e.m. $P<0.05$ compared with *PBS; ‡Flu; §HDM, respectively. H&E, hematoxylin and eosin; HDM, house dust mite; PBS, phosphate-buffered saline; p.i., post infection.

When we examined T-cell populations, mice infected with influenza virus exhibited marked increases in CD8$^+$ but not in CD4$^+$T cells (**Figure 4a** and **b**). In addition, influenza-infected, but not HDM-exposed, mice exhibited significantly increased numbers of activated (CD69$^+$) CD4$^+$ and CD8$^+$ T cells 7 days p.i. Activated CD8$^+$ T cells were markedly increased (24-fold) over PBS-treated mice, whereas the numbers of activated CD4$^+$ T cells were doubled (2.4-fold increase). Furthermore, influenza infection led to an increase (2.3-fold) in T1/ST2$^+$ CD4$^+$ T cells, a cell surface marker specific for the induction of Th2 cells. Finally, we found that DX5$^+$CD3$^+$ cells (NK-T cells) were also dramatically increased in influenza-infected mice (25-fold) (**Figure 4c**). No significant changes on any of these T-cell subsets were observed in infant mice exposed to HDM.

Associated with the dramatic increase in APC and T-cell populations, evaluation of tissue histopathology (at 2 weeks of age) revealed substantial recruitment of inflammatory cells into the lung parenchyma in mice exposed to influenza A at 8 days of age (**Figure 5a**). On the basis of these observations, we next investigated the effector profile induced by an influenza infection in the lungs of neonatal mice. A wide array of cytokines was assessed in lung homogenates on days 3, 5, and 7 after infection of 8-day-old mice. Antiviral, pro-inflammatory, Th1, Th2, and Th17 cytokines, as well as additional cytokines associated with the promotion of Th2 responses (granulocyte macrophage colony-stimulating factor, TSLP, IL-33, IL-25) were all significantly increased with different kinetics during the examination interval (**Figure 5b**). Finally, we examined the levels of TGF-β1 following flu infection. Although we observed a trend for increased expression at 5 days p.i., this increase was not statistically significant (data not shown).

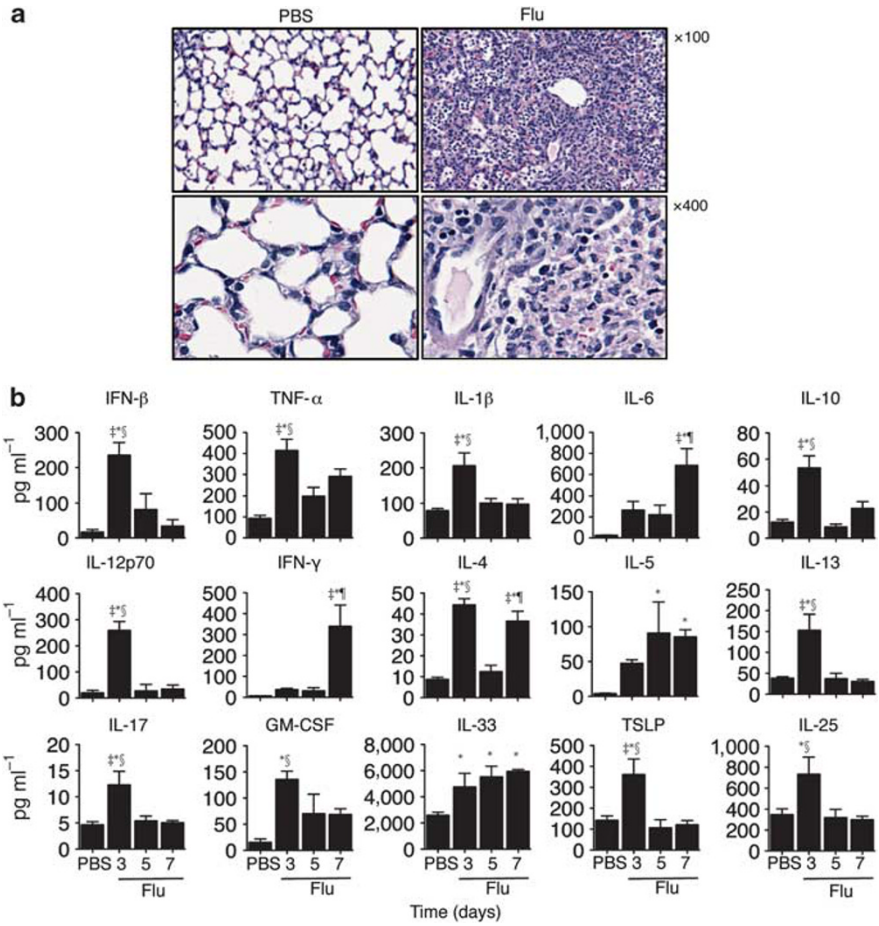

Figure 5 Lung histopathology and cytokine production following influenza A infection in neonatal mice. Groups of 8-day-old mice were either infected with influenza A, PBS treated, or exposed to HDM for 7 consecutive days. (**a**) Lung histopathology was evaluated by H&E to show the degree of immune cell recruitment into the lung parenchyma. All images taken at ×100 and ×400 total magnification as indicated. (**b**) The lungs were isolated at days 3, 5, and 7 p.i., following influenza A infection and kinetics of IFN-β, pro-inflammatory, Th1, Th2, and Th17 cytokines evaluated in lung homogenates. $n=3$–5 mice per group. Data represent mean±s.e.m. $P<0.05$ compared with *PBS, ¶d3, ‡d5, and §d7, respectively. H&E, hematoxylin and eosin; HDM, house dust mite; IFN-β, interferon-β; PBS, phosphate-buffered saline; p.i., post infection.

HDM-specific Th cytokine production in splenocytes following influenza A infection

To determine whether early-life influenza A infection facilitated subsequent HDM-specific T-cell responsiveness, we evaluated T-cell effector function in splenocytes by measuring the production of Th1-, Th2-, and Th17-associated cytokines after restimulation *in vitro* (**Figure 6**). Our data show significantly elevated levels of the Th2-associated cytokines IL-4, IL-5, and IL-13, as well as a 10-fold increase in IL-6 levels in mice concurrently exposed to influenza A and HDM in early life over HDM alone. Similar to Th2 cytokines, modest levels of IL-17 were detected in mice exposed to HDM only, which were significantly increased in mice exposed to influenza A and HDM. In contrast, interferon-γ levels were significantly elevated in both HDM- and HDM-influenza exposed mice with no significant differences between these two groups.

Impact of influenza A infection on structural remodeling in early life

To investigate whether concurrent influenza A infection and HDM exposure in early life promotes the development of airway structural changes, we evaluated goblet cell hyperplasia (mucus production), subepithelial collagen deposition, and smooth muscle thickness (**Figure 7a**). A significant increase in goblet cell hyperplasia (**Figure 7b**) and peribronchial collagen deposition (**Figure 7c**) was detected only in mice exposed to HDM in the context of an influenza infection. In contrast, we did not observe significant differences in peribronchiolar smooth muscle thickness among the treatment groups (**Figure 7d**). Along with these histological changes, we detected significant increases in the levels of the growth factors, TGF-β, $PDGF_{AA}$, and vascular endothelial growth factor only in those mice that had been infected with influenza and concurrently exposed to HDM (**Figure 7e**).

Impact of influenza A infection in early life on structural remodeling in adult life

To determine whether the airway remodeling changes observed after 3 weeks of HDM exposure (5-week-old mice) were dependent on continued allergen exposure, we suspended exposure for an additional 3 weeks (**Figure 8a**). At this point in time (8-week-old mice), tissue and BAL inflammation were resolved

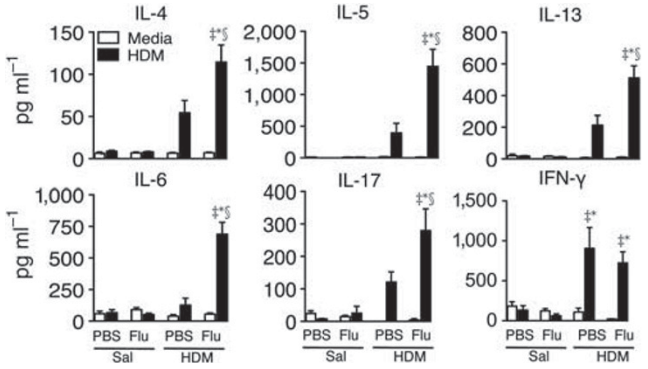

Figure 6 Impact of influenza A infection on house dust mite-specific Th-cytokine responses. Separate groups of 8-day-old mice were infected with influenza virus or given PBS alone. Seven days later, PBS- and Flu-infected groups are exposed either to 3 weeks of HDM or Sal and killed 72 h after the last HDM exposure. Splenocytes from individual mice were cultured in medium alone (□) or stimulated with HDM *in vitro* (■) and Th1-, Th2-, and Th17-associated cytokine production measured by ELISA. For all data, $n=4$–10 mice per group. Data represent mean± s.e.m. $P<0.05$ compared with *Sal, ‡Flu, and §HDM, respectively. ELISA, enzyme-linked immunosorbent assay; HDM, house dust mite; PBS, phosphate-buffered saline.

and the residual inflammation observed in influenza-infected mice was largely mononuclear in nature (**Supplementary Figure 4a** and **b** online). In contrast, HDM-specific immunoglobulin levels remained significantly elevated in mice that had been infected with influenza and exposed to HDM during infancy. As expected, influenza-specific immunoglobulins remained elevated (**Supplementary Figure 4c** online). Our data show that only animals infected with influenza virus and exposed to HDM early in life still exhibited significantly increased mucus production and subepithelial collagen deposition after 3 weeks of allergen discontinuance (**Figure 8b** and **c**). Whereas infant mice infected with influenza virus only did not exhibit increased collagen deposition at 5 weeks of age, a significant increase was observed in this parameter at 8 weeks of age (**Figure 8d**).

In light of the histopathological changes observed, we investigated whether remodeling extended to the parenchymal compartment. We detected an increased number of α-smooth muscle actin (α-SMA)-positive cells, likely representing myofibroblasts, only in animals exposed to HDM in the context of an influenza infection during infancy (**Figure 9a–c** and **e**). Combined staining of α-SMA and the pro-collagen peptide PINP revealed

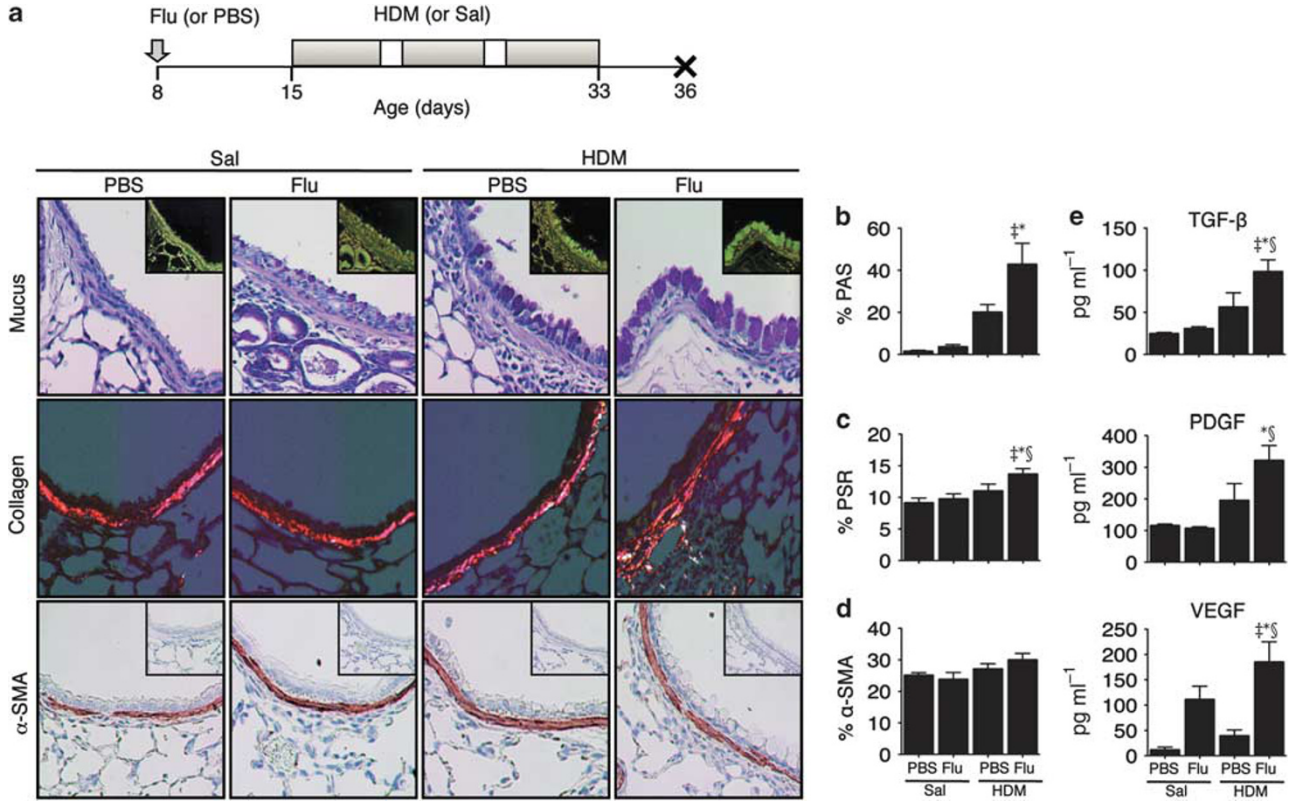

Figure 7 Impact of influenza A infection on airway remodeling in early life. (**a**) Separate groups of 8-day-old mice were infected with influenza virus or given PBS alone. Seven days later, PBS- and Flu-infected groups are exposed either to 3 weeks of HDM or Sal and killed 72 h after the last HDM exposure. Images are representative light photomicrographs of paraffin-embedded cross-sections of lung tissues obtained 72 h after the last HDM exposure. Histopathology was evaluated by (**b**) periodic-acid-Schiff (PAS) staining indicating mucus production of epithelial goblet cells (magenta; insets show color-inverted image used for morphometric analysis); (**c**) Picro Sirus Red (PSR) staining visualized under polarized light indicating subepithelial collagen deposition, and (**d**) Immunohistochemistry for α-smooth muscle actin (α-SMA), indicating contractile elements in the airway wall (brown; insets show nonspecific staining in the corresponding negative control section). (**e**) Remodeling associated growth factors TGF-β, $PDGF_{AA}$, and VEGF in BAL as evaluated by ELISA. All images were taken at ×200 total magnification. For all data, $n=8$–10 mice per group. One of two representative experiments is shown. Data represent mean±s.e.m. $P<0.05$ compared with *Sal, ‡Flu, and §HDM, respectively. ELISA, enzyme-linked immunosorbent assay; HDM, house dust mite; PBS, phosphate-buffered saline; TGF-β, transforming growth factor-β.

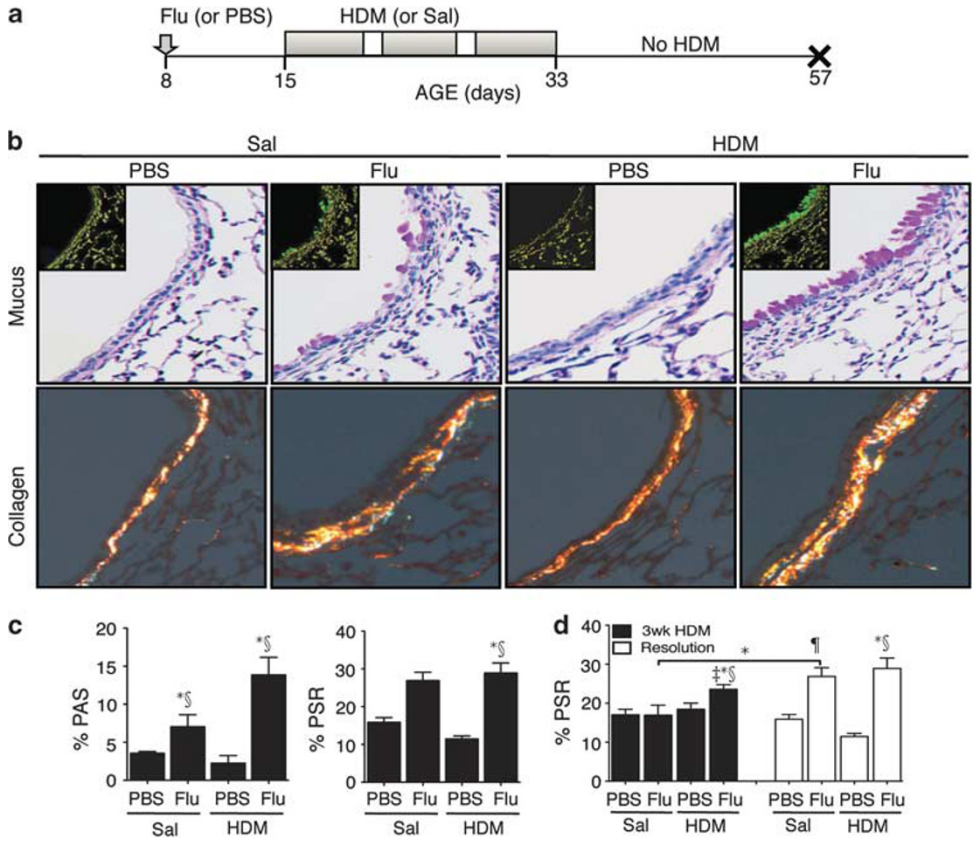

Figure 8 Impact of influenza A infection on airway remodeling in adulthood. (**a**) Separate groups of 8-day-old mice were infected with influenza virus or given PBS alone. Seven days later, PBS- and Flu-infected groups are exposed either to 3 weeks of HDM or Sal, then, after the last HDM exposure, mice were rested for 3 weeks and killed at 8 weeks of age. Images are representative light photomicrographs of paraffin-embedded cross-sections of lung tissue. Lung histopathology as evaluated by (**b**) periodic-acid-Schiff (PAS) staining indicating mucus production of epithelial goblet cells (magenta; insets show color-inverted image used for morphometric analysis) and Picro Sirus Red (PSR) staining visualized under polarized light indicating subepithelial collagen deposition. (**c**) Morphometric analysis of PAS and PSR tissues. (**d**) Comparison of PSR tissues after 3 weeks of HDM exposure or after additional 3 weeks cessation (resolution). All images were taken at ×200 total magnification. For all data, $n=8$–10 mice per group. Data represent mean±s.e.m. $P<0.05$ compared with *Sal, ‡Flu, and §HDM, respectively. HDM, house dust mite; PBS, phosphate-buffered saline.

ongoing collagen synthesis among α-SMA-positive cells in patchy regions of aggravated and cell-rich alveolar inflammation (**Figure 9d**).

Impact of influenza A infection in early life on lung mechanics in adulthood

Finally, we examined whether the changes in airway and parenchymal remodeling that persist into adulthood, led to altered lung function by evaluating respiratory mechanics, specifically airway resistance (R_N), tissue resistance (G), and tissue elastance (H_{TE}). Only mice infected with influenza A and exposed to HDM during infancy exhibited a marked functional impairment as measured by significant increases in R_N, G, and H_{TE} (**Figure 10a** and **b**).

DISCUSSION

A fundamental question regarding AA is the elucidation of its origins. Most cases of AA initiate during early childhood. Given the ubiquitous presence of allergen, it is unlikely that allergen exposure alone may explain its emergence in many instances. In this study, we have investigated the impact of concurrent viral infection and allergen exposure in early life and its impact on the development of allergic airway disease later in life. Prospective birth cohort studies have shown that respiratory viral infections and allergic sensitization in early life are independent risk factors for the development of asthma. Yet, a causal link between these two risk factors and AA has not been established. Respiratory viruses predominantly associated with severe lower respiratory illness and asthma in young children include Respiratory Syncytial Virus and Rhinovirus. However, advances in viral detection methods have identified additional viral types as etiological agents of severe lower respiratory illness's in infants, such as influenza A, human metapneumovirus, and adenovirus among others. Of these, influenza A virus is a significant cause of severe lower respiratory illness in young children that frequently leads to hospitalization.[19] At present, the role that severe influenza A-induced bronchiolitis in infants may have in the generation of asthma has not been clarified.

Several experimental studies have examined the impact of influenza A infections on allergic airway disease in adult mice with divergent outcomes.[20–22] These studies need to be taken with circumspection with regard to their relevance to the

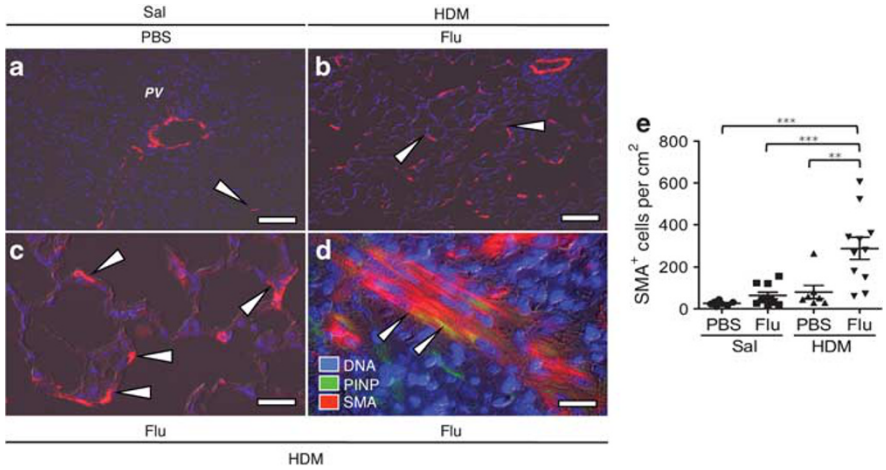

Figure 9 Impact of influenza A infection on parenchymal remodeling in adulthood. Groups of 8-day-old mice were infected with influenza virus or given PBS alone. Seven days later, PBS- and Flu-infected groups are exposed either to 3 weeks of HDM or Sal, then, after the last HDM exposure, mice were rested for 3 weeks and killed at 8 weeks of age. Pictures show immunofluorescence images of α-SMA$^+$ alveolar cells (arrow heads) in the lungs from (**a**) saline and (**b**) influenza and HDM-treated mice. (**c**) Higher magnification reveals the interstitial distribution of the alveolar α-SMA cells in influenza and HDM-treated mice. (**d**) Combined staining for α-SMA and the pro-collagen peptide PINP revealed ongoing collagen synthesis among α-SMA-positive cells in patchy regions of aggravated and cell-rich alveolar inflammation. (**e**) Quantification of α-SMA-positive alveolar cells parenchymal tissue of 8 week-old mice. Scale bars in panels **a** and **b** = 100 μm; panel **c** = 35 μm; panel **d** = 15 μm. *n* = 8–10 mice per group. Data represent mean± s.e.m. $^{**}P<0.01$; $^{***}P<0.001$. α-SMA, α-smooth muscle actin; HDM, house dust mite; PBS, phosphate-buffered saline; PV, pulmonary vessel.

neonatal period because the developing immune system is functionally different from that of adults.[23] In addition, two recent studies have examined whether a respiratory viral infection in early life would affect sensitization initiated in adulthood to the innocuous protein ovalbumin (OVA).[24,25] By design, these studies precluded examining whether an acute viral infection and concurrent aeroallergen exposure in early life leads to allergic sensitization and an asthmatic phenotype in adulthood. The study we report here models a very defined paradigm, which we believe is clinically very relevant. This paradigm encompasses several central features: (i) exposure to a naturally occurring aeroallergen exclusively through the respiratory mucosa, (ii) exposure to such aeroallergen concurrently with an ongoing respiratory viral infection, and (iii) focus on the initiation of these perturbations at a clinically relevant developmental time frame (approximately equivalent to the first 2 years of life in humans).

We established a model of respiratory mucosal sensitization using HDM, the most pervasive indoor allergen worldwide, and which does not require the use of additional exogenous adjuvants. In accordance with our previous data,[26] exposure to a high dose of HDM for 3 weeks elicits, in adult mice, substantial airway inflammation and robust eosinophilia. In sharp contrast, infant mice exhibit minimal immuno-responsiveness to HDM as evidenced by reduced BAL and tissue inflammation, including minimal recruitment of eosinophils, absence of allergen-specific immunoglobulins, and minimal Th2 cytokine responses. Failure to respond to such an intrinsically allergenic material[27] suggests that allergen exposure in early life is, by itself, insufficient to generate allergen-specific sensitization and allergic airway inflammation. The homeostatic mechanisms mediating HDM hyporesponsiveness at this period of development likely encompass a complex network of regulatory immune pathways.[28,29] We provide evidence that, in the steady state, infant mice have elevated levels of TGF-β and IL-10 in the lungs, two cytokines with powerful regulatory and immunosuppressive activities.[30,31] Whether these are the only regulatory cytokines involved, the cellular source of these cytokines, the specific mechanisms of action, and the contribution from the mother to allergen hyporesponsiveness, through regulatory molecules present in the milk[32] are, among others, interconnected questions, the elucidation of which is beyond the scope of this study. Our research aimed to investigate whether a severe viral infection in infancy was able to overcome constitutive allergen hyporesponsiveness and the proximal and remote consequences of this effect. Our data clearly demonstrate that an acute infection with influenza A perturbs the lung in such a way as to enable allergen responsiveness as assessed by every parameter studied: airway inflammation, HDM-specific immunoglobulins, and systemic Th2 immunity. There is evidence that suggests that neonatal animals generate only mild inflammatory responses to inhaled antigens such as OVA and cockroach extracts,[33–35] and that co-exposure to air pollution,[33] endotoxin,[34] or bacterial and viral TLR ligands[35] significantly enhances inflammatory responses. Thus, our data are in line with the concept that sensitization to a pervasive allergen in early life and generation of asthma later on, depends on immunological perturbations brought about by concurrent exposures, such as severe viral infections.[5,36]

In contrast to the remarkable hyporesponsiveness to HDM, neonates respond, similar to adults, to a potentially life-threatening encounter such as influenza A infection. To gain insights into the immunological mechanisms underlying the divergent responses to HDM and influenza A, we investigated the status of the APC compartment. Our data show that influenza A infection led to recruitment and activation of NK cells, Ly6C^{hi}

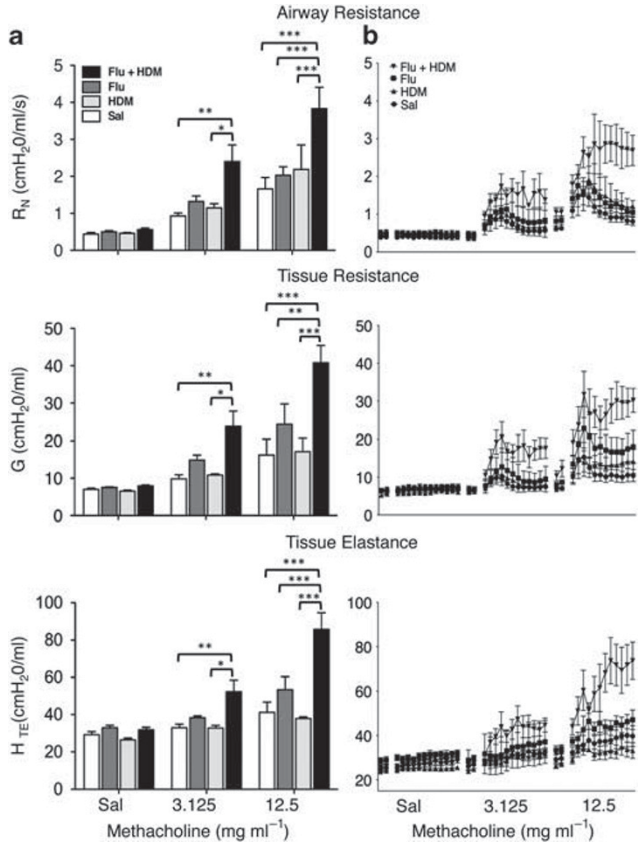

Figure 10 Impact of influenza A infection in early life on lung mechanics later in life. Groups of 8-day-old mice were infected with influenza virus or given PBS alone. Seven days later, PBS- and Flu-infected groups are exposed either to 3 weeks of HDM or Sal, then, after the last HDM exposure, mice were rested for 3 weeks and killed at 8 weeks of age and lung function evaluated. Airway responsiveness to increasing doses of methacholine was assessed for R_N, G, and H_{TE} and is shown (**a**) as maximum R_N, G, and H_{TE}, and, (**b**) as time course of 12 consecutive measurements. For all data, $n=8$–10 mice per group. Data represent mean±s.e.m. *$P<0.05$, **$P<0.01$, ***$P<0.001$; two-way ANOVA (Bonferroni's *post hoc* test). ANOVA, analysis of variance; HDM, house dust mite; PBS, phosphate-buffered saline.

monocytes and iDCs, as well as two pDCs subtypes; these events led to robust $CD4^+$ and $CD8^+$ T-cell responses. In comparison with influenza A, HDM exposure (in neonates) led to significant increases only in alveolar macrophages; however, these changes did not lead to significant increases in the number or activation state of $CD4^+$ and $CD8^+$ T cells. Interestingly, similar to influenza A, only adult, and not neonatal mice exposed to HDM exhibited significantly increased numbers of iDCs and $CD8\alpha^+$ pDCs suggesting that these two cell populations may have a critical role in driving immune-inflammatory responses to HDM. Whereas, iDCs are recruited to the lung for the production of inflammatory cytokines,[18] and are necessary for HDM-mediated inflammation in adult mice,[37] $CD8\alpha^+$ pDCs represent an activated pDC subtype involved in the generation of type I interferon and have been shown to emerge after microbial exposure.[14,16] Collectively, these data suggest that HDM exposure in neonatal mice had, with the exception of alveolar macrophages, a negligible impact on APC subsets in the lung, and further reveal that influenza infection in neonatal mice leads to the recruitment of specific APC subtypes such as iDCs and activated pDCs, which may be critical for HDM responsiveness.

To provide further mechanistic insights into the effects of influenza A infection that may facilitate allergen responsiveness, we investigated the expression of several members of the TLR family. Whereas HDM exposure in neonates did not increase TLR expression, influenza A infection did. Among those TLRs the expression of which was increased, TLR4 is particularly relevant as it has been directly implicated in HDM-mediated inflammation in adult mice.[38–40]

The efficient recognition of and rapid host response to influenza infection led to extensive infiltration of immune-inflammatory cells into the lung parenchyma resulting in acute bronchiolitis-like pathology resembling that observed in human infants infected with respiratory syncytial virus or influenza A virus.[41] As a result, the environment encountered by HDM in a lung undergoing a severe influenza infection is exceptionally rich in immune mediators. Although influenza A virus is considered an archetypic Th1-inducing signal, the effector profile that we demonstrate in neonates defies dichotomous categorizations (i.e., Th1 vs. Th2). In fact, influenza A induced an increased expression of both Th1 and Th2, as well as Th17 and a number of pro-inflammatory and anti-viral cytokines. Moreover, we observed increased production of cytokines capable of promoting Th2 immunity (granulocyte macrophage colony-stimulating factor, IL-25, IL-33, and TSLP).[42] Evidence of such a prolific effector response intimates that the viral-mediated acquisition of allergen responsiveness in the neonatal setting is unlikely mediated by a single molecular signal but, rather, by a community of cytokines.

From a mechanistic perspective, our data show that influenza A infection led to a heightened state of immune alertness, encompassing the activation of multiple cellular components and pathways, as well as the production of many immune mediators; we propose that this pervasive priming of the lung environment reduced the threshold necessary to trigger allergen responsiveness. These findings prompt a critical appraisal of a prevailing theory regarding the development of asthma. Indeed, according to the Hygiene Hypothesis, exposure to microbial agents in early life results in protective immunity against allergic disease.[43] Yet, we demonstrate that exposure to influenza A virus in early life overcomes constitutive allergen hyporesponsiveness and primes the lung environment to facilitate allergic responses. These findings expose the shortcomings of the Hygiene Hypothesis to account for the likely diverse consequences of distinctive microbial exposures in early life.

Structural abnormalities of the airway, collectively referred to as remodeling, are believed to contribute to airway dysfunction, the cardinal feature of asthma. The conventional paradigm is that remodeling is secondary to chronic inflammation. However, several features of remodeling have been observed in very young children with a diagnosis of asthma.[44] Moreover, Saglani *et al.*[45] have shown that changes in remodeling can be detected in children with persistent wheeze as young as 3 years of age. These findings have led to the suggestion that

inflammation and remodeling may be independent processes.[46] Yet, the link between remodeling and inflammation in young children remains tenuous, in part, because, in humans, it is difficult to track back with precision the individual's immune-inflammatory history.

Our study demonstrates that HDM exposure in very young mice leads to airway remodeling only when robust allergic inflammation, facilitated by a single severe event, such as that caused by an influenza infection, was elicited. Interestingly, these airway remodeling changes occurred at an accelerated pace as compared with adults,[47] and importantly, persisted after a prolonged period of cessation of allergen exposure. Translationally, our data advocate that influenza A infections, and, likely, other viral infections associated with severe bronchiolitis in early life may propel allergic airway remodeling, and that these structural changes could persist in young adults, even if inflammation is no longer present.

The pathology exhibited by mice exposed to HDM while undergoing an influenza A infection clearly extends beyond the airway and into the lung parenchyma. A closer examination of this compartment revealed a dramatic increase in the number of alveolar α-SMA$^+$ cells, similar to a finding reported in OVA-sensitized and OVA-challenged mice.[48] To the best of our knowledge, there are no studies in human asthma that have examined parenchymal remodeling. Interestingly, α-SMA$^+$ cells express muscarinic receptors and, hence are capable of responding to methacholine and contribute to airway hyperreactivity.[49,50] In this regard, we evaluated the long-term impact of concurrent viral and allergen exposure on the generation of airway hyperreactivity. Our data demonstrate that even after prolonged cessation of allergen exposure and, effectively, absent airway inflammation, airway resistance (R_N), tissue resistance (G), and tissue elastance (H), all indicators of airway closure in response to methacholine challenge,[51] were markedly elevated only in those, now adult, mice that had been exposed to HDM in the context of an influenza A infection during infancy. Thus, our findings underscore the long-lasting impact allergen exposure has on lung function at a time of a severe viral infection in early life. The precise links between inflammation, structural changes, and functional alterations remain obscure in both humans and experimental systems. Our data show that marked alterations in respiratory mechanics are evident when there is no longer inflammation but there is mucus metaplasia, an increase in parenchymal myofibroblasts, as well as increased subepithelial collagen deposition. With regard to the latter, such a feature is also detected in adult mice that were infected with influenza A (only) in early life; yet this is not associated with significant alterations in respiratory mechanics, suggesting that, at least in this system, increased subepithelial collagen deposition alone does not lead, by itself, to functional impairment.

Understanding the origins of AA remains elusive. Unfortunately, genetic studies to date have been plagued by inconsistencies and poor reproducibility across populations. As proposed by Guerra and Martinez,[52] meaningful progress requires an approach that integrates interactive influences from the environment, biological systems, and developmental processes.[53] Here, we have developed a model that encompasses: (i) the use of a relevant aeroallergen capable of inducing a response when delivered mucosally in the absence of additional adjuvants, (ii) an environmental disturbance of the system in the form of an influenza A infection at the time of allergen exposure, and (iii) a relevant developmental interval as, in most instances, AA develops in humans within the first few years of life. Our data demonstrate that a severe immune perturbation in early life, such as that caused by a severe influenza A infection, can subvert the responsiveness to an otherwise harmless allergen leading to the expression of an AA phenotype in adulthood. In a broader context, these findings intimate the notion that diverse microbial exposures may have distinctive consequences: protection from vs. promotion of allergic disease. We would speculate that the severity of the acute immune-inflammatory response, rather than the nature of the initiating immune signal, is the variable that determines a detrimental outcome. Importantly, our study suggests that interventions to reduce the lung inflammation caused by such events may be essential in preventing subsequent allergen sensitization and asthma in the youngest population.

METHODS

Animals. Fifteen-day pregnant (female) BALB/c mice were purchased from Charles River Laboratories (Ottawa, ON, Canada) and housed under specific pathogen-free conditions and maintained on a 12-h light–dark cycle with food and water *ad libitum*. Upon birth, mothers were housed with their litters in light-protected cages until completion of the study (or weaning at 4 weeks of age). All experiments described in this study were approved by the Animal Research Ethics Board of McMaster University (Hamilton, ON, Canada).

Influenza A infection and sensitization protocols. Separate groups of 8-day-old BALB/c mice were infected without anesthesia with either influenza A/PR8 virus or PBS solution. Influenza type A virus strain A/PR/8/34 (H1N1) was prepared as described previously.[20] The viral stock suspension (10^9 PFU ml^{-1}) was diluted 6,000-fold and a sublethal dose of ~1 PFU administered intranasally in 15 µl PBS.

Allergen administration: HDM extract (Greer Laboratories, Lenoir, NC) was resuspended in sterile saline (Sal) at a concentration of 2.5 µg (protein) per µl and 10 µl (25 µg dose) was administered to lightly isofluorane-anesthetized 2- and 8-week-old mice by intranasal delivery. According to the manufacturer, the levels of endotoxin in HDM extracts range between 25 and 100 EU ml^{-1} extract; this corresponds to 0.25–1 EU per dose of allergen per day or 0.1–1 ng per 25 µg dose. These levels of lipopolysaccharide are significantly lower than the 100 ng dose of lipopolysaccharide required to promote Th2 responses in OVA models of allergic disease.[54]

Concurrent influenza A infection and allergen exposure in early life: Groups of 8-day-old mice were infected with influenza A or PBS and then 7 days later, groups of mice were exposed either to HDM or Sal, 5 days a week for a total of 3 weeks. The immune-inflammatory response and structural changes were evaluated 3 days after the last challenge (**Figure 2a**).

Airway inflammation and remodeling in adulthood: To investigate whether structural changes persisted, the protocol was recapitulated and, after the last allergen challenge, mice were allowed to rest for a period of 3 weeks (**Figure 8a**). The inflammatory and remodeling responses were re-evaluated and the impact on lung mechanics determined.

Immune activation after influenza A infection or allergen exposure: To examine the difference in immune activation in neonatal mice exposed to HDM or infected with influenza, groups of 8-day-old mice were infected with either flu virus or exposed to 7 doses of HDM or PBS

and an identical dose of HDM administered to adult mice. The immune-inflammatory response was evaluated in the lungs 24 h after the last challenge or at day 7 p.i.

Collection and measurement of specimens. BAL fluid, lungs, and blood were collected at the time of killing. BAL was performed as described previously.[20] In brief, the lungs were dissected and the trachea cannulated using a polyethylene tube (outer/inner diameter = 0.965/0.58 mm; Becton Dickinson, Sparks, MD). The lungs were lavaged twice with PBS (0.25 ml followed by 0.2 ml), and approximately 0.25–0.3 ml of the instilled fluid was retrieved consistently. Total cell counts were then determined using a hemocytometer. Each BAL sample was then centrifuged and the supernatants collected and stored at −20°C. Cell pellets were subsequently resuspended in PBS and cytospins were prepared by centrifugation (Shandon, Pittsburgh, PA) at 300 r.p.m. for 2 min. Protocol Hema 3 stain set (Fisher Scientific, Toronto, ON, Canada) was used to stain all smears. Differential cell counts of BAL were determined from at least 300 leukocytes using standard hemocytological criteria to classify the cells as neutrophils, eosinophils, or mononuclear cells. Peripheral blood was collected by retro-orbital bleeding, and serum was obtained and stored at −20°C. Harvested spleens were placed in sterile tubes containing sterile Hank's balanced salt solution. Where applicable, after BAL collection, the lungs were inflated with 10% formalin at constant pressure of 20 cm H_2O and then fixed in 10% formalin for 48–72 h until further processing. For some measurements, the lungs were dissected without previous BAL collection and placed in PBS at 4°C for tissue homogenate preparation or snap frozen in liquid nitrogen for RNA isolation and quantitative real-time PCR assay.

Histology and immunohistochemistry. After formalin fixation, the left lung was dissected and embedded in paraffin. Sections of 3-μm thickness were cut and stained with hematoxylin and eosin, Picro Sirius Red, or periodic acid-Schiff. Immunohistochemistry for α-SMA was also performed as described previously.[20,55] Images stained with hematoxylin and eosin were captured through Leica camera and microscope (Leica Microsystems, Richmond Hill, ON, Canada) with the magnification of the objective adjusted, as necessary, from ×5 to ×40. For all experiments, the eye piece remained constant at ×10, achieving total magnifications ranging from ×50 to ×400.

Morphometric analysis. Images for morphometric analysis were captured using OpenLab software (v3.0.3; Improvision, Guelph, ON, Canada) using Leica camera and microscope (Leica Microsystems). Image analysis was performed using a custom-computerized analysis system (Northern Eclipse software version 5; Empix Imaging, Mississauga, ON, Canada). Analysis of sections stained for α-SMA, Picro Sirius Red, and periodic acid-Schiff-stained sections were performed as described previously.[20,55] Distances of 20 and 40 μm (starting from below the airway epithelium and proceeding away from the lumen) were used for α-SMA and Picro Sirius Red images, respectively, whereas a distance of 30 μm (starting from below the airway epithelium and proceeding toward the lumen) was used for periodic acid-Schiff-stained images. All images were captured with the objective lens set to a magnification power of ×20 and the eye piece set to ×10, achieving a total magnification of ×200.

Preparation of lung tissue homogenate. Whole lungs were homogenized in 1.5 ml PBS supplemented with 1 COMPLETE protease inhibitor tablet (Roche, Laval, QC, Canada) per 10 ml of buffer. After homogenization, 150 μl of 10% Triton X-100 was added and samples were rocked at 4°C for 1 h. The supernatant was collected following a 15 min spin at 12,000 r.p.m. at 4°C and stored at −70°C.

RNA isolation and quantitative real-time PCR. Total RNA was extracted from frozen lung tissues using RNA-STAT60 reagent (Tel-Test, Friendwood, TX) as per the manufacturer's protocol. The extracted total RNA was further purified using RNeasy Mini Kit (Qiagen, Valencia, CA) and the quality assessed using the Agilent Bioanalyzer 2,100 (Agilent, Santa Clara, CA). Total RNA quantities were determined and 2 μg used for first-strand cDNA synthesis using TaqMan reverse transcriptase-PCR kit as per the manufacturer's protocol. Primer and probe sets for murine TLR 2, 3, 4 5, 7, and 9, and 18 sRNA (internal control) were chosen from Applied Biosystem's Pre-Developed TaqMan Assay reagents (Applied Biosystems, Foster City, CA) and mRNA expression profiles analyzed using ABI-7900HT. Each sample was normalized to the expression of 18sRNA. Relative expression levels were determined using the equation $2^{-\Delta\Delta Ct}$ (within Applied Biosystems Sequence Detection software version 2.2.1).

Lung cell isolation and flow cytometric analysis of lung cells. Total lung cells were isolated as described previously.[20] In brief, total lung cells were isolated by collagenase digestion (Collagenase type I; Life Technologies, Burlington, ON, Canada) washed twice in fluorescence-activated cell sorting buffer (PBS/0.5% bovine serum albumin), and then filtered through 40-μm cell strainer and stained with a panel of antibodies for analysis by 13-color flow cytometry. For each antibody combination, 2×10^6cells were incubated with monoclonal antibodies at 4°C for 30 min. Cells were then washed in fluorescence-activated cell sorting buffer, counted to obtain total cells, and data were collected using an LSRII flow cytometer (BD, Franklin Lakes, NJ). More than 300,000 events were collected for each group. Immune cells were analyzed using FlowJo software (Tree Star, Ashland, OR). The following antibodies were used for identification of intraepithelial DCs, iDCs, alveolar macrophages, pDC, act pDC, Ly6C^{hi} monocytes, B cells, and NK cells: CD45-allophyocyanine-Cyanine(Cy)7, CD3-Pacific Blue, CD11c-fluorescein isothiocyanate, F4/80-phycoerythrin (PE)-Cy5 (all BD Bioscience, Mississauga, ON, Canada), major histocompatibility complex II-Alexa Fluor 700, CD11b-PE, Ly6c-Peridinin Chlorophyll Protein Complex-Cy5.5, DX5-PE-Cy7, and SiglecH-Alexa Fluor 647 (all eBioscience, San Diego, CA). CD8α-PE-Alexa Fluor 610, GR1-Pacific Orange, and CD4-Qdot605 (all Invitrogen, Carlsbad, CA) and mPDCA-1-allophyocyanine (Miltenyi Biotech, Auburn, CA). For some experiments, B220-Qdot800 (strepdavidin) or CD86-Qdot800 (strepdavidin) (BD Bioscience) and B220-Qdot655 or CD86-PE-Cy7 (eBioscience) were used interchangeably. T cells were identified using CD3-Pacific Blue, CD4-allophyocyanine, CD8-PE, CD69-PE-Cy7, CD45-allophyocyanine-Cy7 (all BD Bioscience), and T1/ST2- fluorescein isothiocyanate (MD Bioscience, St Paul, MN). All appropriate isotype controls and fluorescent minus one controls were used. Antibodies were titrated to determine optimal concentration. See **Supplementary Figures 1** and **2** online for gating strategy used to identify allophyocyanines and additional details on the methods used to make these measurements.

Splenocyte cultures. Splenocytes were isolated and resuspended in complete RPMI at a concentration of 8×10^6 cells per ml as described previously.[55] In brief, cells were cultured in medium alone or with the medium supplemented with HDM (31.25 μg ml^{-1}) in a flat-bottom, 96-well plate (Becton Dickinson, Mississauga, ON, Canada) in triplicate. After 5 days of culture, supernatants were harvested and triplicate samples were pooled for cytokine measurements.

Cytokine analysis and immunoglobulin measurements. Cytokines levels were measured in lung homogenates and supernatants of splenocyte cultures using Luminex 100 Total System (Luminex, Austin, TX) based on xMAPmultiplexing technology. 9-Plex cytokine kits containing microbeads with capture antibody and biotinylated reporter specific for mouse IL-1β, IL-4, IL-5, IL-6, IL-10, IL-13, IL-17, interferon-γ, and granulocyte macrophage colony-stimulating factor were purchased from Upstate (Charlottesville, VA), whereas type I interferon-β was measured using enzyme-linked immunosorbent assay (ELISA) kits purchased from PBL Biomedical Laboratories (Piscataway, NJ). IL-12p70 and IL-33 were measured using eBioscience ELISA kits. TSLP, IL-25, tumor necrosis factor-α, and TGF-β1 were measured using DuoSet ELISA kits (R&D Systems, Minneapolis, MN). Levels of growth factors in BAL were measured for TGF-β1 and vascular endothelial growth factor using DuoSet ELISA kits and for $PDGF_{AA}$ by Quantikine ELISA kits (R&D Systems) and used according to the manufacture's instructions. Levels of Flu IgG_1

and IgG_{2a} and HDM-specific IgE, IgG_1, and IgG_2 were measured by sandwich ELISA as described previously.[20,47] The formula used to calculate relative units = (OD reading – OD blank)×10.

Assessment of alveolar αSMA-positive cells. To detect alveolar α-SMA-positive cells, paraffin sections of 3 μm were immunostained for α-SMA. Sections were deparaffinized, rehydrated, and incubated for 1 h at room temperature with an alkaline phosphatase-conjugated monoclonal antibody against α-SMA (1:200, C5691, clone 1A4, Sigma-Aldrich, Stockholm, Sweden). Immunoreactivity was detected using a permanent red substrate kit (K0640, Dako, Glostrup, Denmark). Sections were counterstained with Mayer's hematoxylin, dehydrated in ethanol, and mounted in Pertex (HistoLab, Gothenburg, Sweden). High-resolution digital images of whole-lung tissue sections were generated using Aperio ScanScope slide scanner (Aperio Technologies, Vista, CA). The alveolar parenchyma, excluding small airways and pulmonary vessels, were delineated by freehand using image analysis (ImageScope software, Aperio Technologies), and the total number of $\alpha\text{-SMA}^+$ cells per cm^2 alveolar parenchyma was quantified on blinded sections. Double-staining immunofluorescence was performed for the identification of $\alpha\text{-SMA}^+$ cells co-expressing procollagen I (PINP) and α-SMA. After enzymatic retrieval with pepsin/HCl (0.4% pepsin in 0.01 M HCl) for 20 min in 37°C, paraffin sections were blocked with 10% normal goat serum (Sigma, Munich, Germany) for 20 min. Sections were then incubated overnight at 4°C with a rabbit polyclonal antibody against PINP (1:300, gift from J Risteli and J Karttunen, Oulu University, Finland), followed by incubation for 1 h at room temperature with Alexa 488-conjugated goat anti-rabbit secondary antibody (1:200, Invitrogen). A second staining for α-SMA was performed using a Cy3-conjuagted monoclonal antibody against α-SMA (1:1,000, C6198, Sigma-Aldrich). Cell nuclei were stained with Hoechst (H33342, Sigma-Aldrich) and sections mounted in Tris-buffered saline/glycerol. Negative controls were performed by isotype-matched control antibodies.

Airway responsiveness measurements. Airway responsiveness was assessed 30 days after the last exposure to HDM in response to increasing doses of nebulized methacholine (Sigma-Aldrich, Oakville, ON, Canada) using a previously described protocol.[26] In brief, mice were anesthetized with inhaled isoflurane (3% with 1 l min^{-1} of O_2), paralyzed with pancuronium bromide (1 mg intraperitoneal), tracheotomized using a blunted 18-G needle, and mechanically ventilated using a small animal computer-controlled piston ventilator (flexiVent, SCIREQ, Montreal, QC, Canada). Mice received 200 breaths per minute and a tidal volume of 0.25 ml; the respiratory rate was slowed during nebulization (10 s) to provide 5 large breaths of aerosol at a tidal volume of 0.8 ml. The response to nebulized saline and increasing doses (3.125 and 12.5 mg ml) of methacholine was measured and the data fit with the constant phase model. Model parameters of airway resistance (Rn), tissue resistance (G), and tissue elastance (H) were calculated as described previously.[56] Model fits that resulted in a coefficient of determination < 0.08 were excluded.

Data analysis. Data were analyzed using GraphPad Prism (version 5.0; GraphPad, La Jolla, CA) and expressed as mean±s.e.m. Results were interpreted using either one-way analysis of variance and Tukey's *post hoc* test, or two-way analysis of variance and Bonferroni's *post hoc* text. Differences were considered statistically significant when $P < 0.05$.

SUPPLEMENTARY MATERIAL is linked to the online version of the paper at http://www.nature.com/mi

ACKNOWLEDGMENTS

We gratefully acknowledge the technical help of Mary-Jo Smith, Mary Bruni, and Natalia Arias. We also thank Dr Jack Gauldie for careful review of the manuscript and Marie Colbert for administrative assistance.
This research was partially funded by the Canadian Institute of Health Research (CIHR) and MedImmune LLC. AA-G. holds a Scholar Award from King Abdullah University of Science and Technology; RF holds an Ontario Graduate Fellowship; MJ holds a Senior Canada Research Chair in Immunobiology of Respiratory Disease and Allergy.

DISCLOSURE

The authors declare no conflict of interest. AAH and RK are current employees of MedImmune, and AJC is a former employee of MedImmune, LLC.

REFERENCES

1. Asthma (WHO, 2008). Asthma. In Fact Sheet Nº 307 (WHO, 2011).
2. Sigurs, N. *et al.* Severe respiratory syncytial virus bronchiolitis in infancy and asthma and allergy at age 13. *Am. J. Respir. Crit. Care Med.* **171,** 137–141 (2005).
3. Simoes, E.A. Respiratory syncytial virus infection. *Lancet* **354,** 847–852 (1999).
4. Jackson, D.J. *et al.* Wheezing rhinovirus illnesses in early life predict asthma development in high-risk children. *Am. J. Respir. Crit. Care Med.* **178,** 667–672 (2008).
5. Kusel, M.M. *et al.* Early-life respiratory viral infections, atopic sensitization, and risk of subsequent development of persistent asthma. *J. Allergy Clin. Immunol.* **119,** 1105–1110 (2007).
6. Martinez, F.D. *et al.* Asthma and wheezing in the first six years of life. The Group Health Medical Associates. *N. Engl. J. Med.* **332,** 133–138 (1995).
7. Morgan, W.J. *et al.* Outcome of asthma and wheezing in the first 6 years of life: follow-up through adolescence. *Am. J. Respir. Crit. Care Med.* **172,** 1253–1258 (2005).
8. Illi, S. *et al.* Perennial allergen sensitisation early in life and chronic asthma in children: a birth cohort study. *Lancet* **368,** 763–770 (2006).
9. Prevention of influenza: recommendations for influenza immunization of children, 2007–2008. *Pediatrics* **121,** e1016–e1031 (2008).
10. Osterholzer, J.J. *et al.* Accumulation of CD11b+ lung dendritic cells in response to fungal infection results from the CCR2-mediated recruitment and differentiation of Ly-6Chigh monocytes. *J. Immunol.* **183,** 8044–8053 (2009).
11. Vermaelen, K. & Pauwels, R. Accurate and simple discrimination of mouse pulmonary dendritic cell and macrophage populations by flow cytometry: methodology and new insights. *Cytometry A* **61,** 170–177 (2004).
12. GeurtsvanKessel, C.H. *et al.* Clearance of influenza virus from the lung depends on migratory langerin+CD11b- but not plasmacytoid dendritic cells. *J. Exp. Med.* **205,** 1621–1634 (2008).
13. Beaty, S.R., Rose, C.E. Jr. & Sung, S.S. Diverse and potent chemokine production by lung CD11bhigh dendritic cells in homeostasis and in allergic lung inflammation. *J. Immunol.* **178,** 1882–1895 (2007).
14. Swiecki, M. & Colonna, M. Unraveling the functions of plasmacytoid dendritic cells during viral infections, autoimmunity, and tolerance. *Immunol. Rev.* **234,** 142–162 (2010).
15. Blasius, A.L., Barchet, W., Cella, M. & Colonna, M. Development and function of murine B220+CD11c+NK1.1+ cells identify them as a subset of NK cells. *J. Exp. Med.* **204,** 2561–2568 (2007).
16. O'Keeffe, M. *et al.* Mouse plasmacytoid cells: long-lived cells, heterogeneous in surface phenotype and function, that differentiate into CD8(+) dendritic cells only after microbial stimulus. *J. Exp. Med.* **196,** 1307–1319 (2002).
17. GeurtsvanKessel, C.H. *et al.* Both conventional and interferon killer dendritic cells have antigen-presenting capacity during influenza virus infection. *PLoS One* **4,** e7187 (2009).
18. GeurtsvanKessel, C.H. & Lambrecht, B.N. Division of labor between dendritic cell subsets of the lung. *Mucosal Immunol.* **1,** 442–450 (2008).
19. Poehling, K.A. *et al.* The underrecognized burden of influenza in young children. *N. Engl. J. Med.* **355,** 31–40 (2006).
20. Al-Garawi, A.A. *et al.* Acute, but not resolved, influenza A infection enhances susceptibility to house dust mite-induced allergic disease. *J. Immunol.* **182,** 3095–3104 (2009).
21. Dahl, M.E., Dabbagh, K., Liggitt, D., Kim, S. & Lewis, D.B. Viral-induced T helper type 1 responses enhance allergic disease by effects on lung dendritic cells. *Nat. Immunol.* **5,** 337–343 (2004).
22. Wohlleben, G. *et al.* Influenza A virus infection inhibits the efficient recruitment of Th2 cells into the airways and the development of airway eosinophilia. *J. Immunol.* **170,** 4601–4611 (2003).
23. Adkins, B., Leclerc, C. & Marshall-Clarke, S. Neonatal adaptive immunity comes of age. *Nat. Rev. Immunol.* **4,** 553–564 (2004).

24. You, D. *et al.* Exposure of neonates to respiratory syncytial virus is critical in determining subsequent airway response in adults. *Respir. Res.* **7,** 107 (2006).
25. Siegle, J.S. *et al.* Early-life viral infection and allergen exposure interact to induce an asthmatic phenotype in mice. *Respir. Res.* **11,** 14 (2010).
26. Llop-Guevara, A. *et al. In vivo*-to-in silico iterations to investigate aeroallergen-host interactions. *PLoS One* **3,** e2426 (2008).
27. Cates, E.C., Fattouh, R., Johnson, J.R., Llop-Guevara, A. & Jordana, M. Modeling responses to respiratory house dust mite exposure. *Contrib. Microbiol.* **14,** 42–67 (2007).
28. Holt, P.G., Strickland, D.H., Wikstrom, M.E. & Jahnsen, F.L. Regulation of immunological homeostasis in the respiratory tract. *Nat. Rev. Immunol.* **8,** 142–152 (2008).
29. Wissinger, E., Goulding, J. & Hussell, T. Immune homeostasis in the respiratory tract and its impact on heterologous infection. *Semin. Immunol.* **21,** 147–155 (2009).
30. Munger, J.S. *et al.* The integrin alpha v beta 6 binds and activates latent TGF beta 1: a mechanism for regulating pulmonary inflammation and fibrosis. *Cell* **96,** 319–328 (1999).
31. Saraiva, M. & O'Garra, A. The regulation of IL-10 production by immune cells. *Nat. Rev. Immunol.* **10,** 170–181 (2011).
32. Mosconi, E. *et al.* Breast milk immune complexes are potent inducers of oral tolerance in neonates and prevent asthma development. *Mucosal Immunol.* **3,** 461–474 (2010).
33. Hamada, K., Goldsmith, C.A., Goldman, A. & Kobzik, L. Resistance of very young mice to inhaled allergen sensitization is overcome by coexposure to an air-pollutant aerosol. *Am. J. Respir. Crit. Care Med.* **161,** 1285–1293 (2000).
34. Kulhankova, K. *et al.* Early-life co-administration of cockroach allergen and endotoxin augments pulmonary and systemic responses. *Clin. Exp. Allergy* **39,** 1069–1079 (2009).
35. Phipps, S. *et al.* Allergic sensitization is enhanced in early life through toll-like receptor 7 activation. *Clin. Exp. Allergy* **39,** 1920–1928 (2009).
36. Holt, P.G., Upham, J.W. & Sly, P.D. Contemporaneous maturation of immunologic and respiratory functions during early childhood: implications for development of asthma prevention strategies. *J. Allergy Clin. Immunol.* **116,** 16–24; quiz 25 (2005).
37. Hammad, H. *et al.* Inflammatory dendritic cells—not basophils—are necessary and sufficient for induction of Th2 immunity to inhaled house dust mite allergen. *J. Exp. Med.* **207,** 2097–2111 (2010).
38. Hammad, H. *et al.* House dust mite allergen induces asthma via Toll-like receptor 4 triggering of airway structural cells. *Nat. Med.* **15,** 410–416 (2009).
39. Trompette, A. *et al.* Allergenicity resulting from functional mimicry of a Toll-like receptor complex protein. *Nature* **457,** 585–588 (2009).
40. Phipps, S. *et al.* Toll/IL-1 signaling is critical for house dust mite-specific helper T cell type 2 and type 17 [corrected] responses. *Am. J. Respir. Crit. Care Med.* **179,** 883–893 (2009).
41. Visscher, D.W. & Myers, J.L. Bronchiolitis: the pathologist's perspective. *Proc. Am. Thorac. Soc.* **3,** 41–47 (2006).
42. Paul, W.E. & Zhu, J. How are T(H)2-type immune responses initiated and amplified? *Nat. Rev. Immunol.* **10,** 225–235 (2010).
43. Strachan, D.P. Hay fever, hygiene, and household size. *B.M.J.* **299,** 1259–1260 (1989).
44. Barbato, A. *et al.* Airway inflammation in childhood asthma. *Am. J. Respir. Crit. Care Med.* **168,** 798–803 (2003).
45. Saglani, S. *et al.* Early detection of airway wall remodeling and eosinophilic inflammation in preschool wheezers. *Am. J. Respir. Crit. Care Med.* **176,** 858–864 (2007).
46. Bush, A. How early do airway inflammation and remodeling occur? *Allergol. Int.* **57,** 11–19 (2008).
47. Johnson, J.R. *et al.* Continuous exposure to house dust mite elicits chronic airway inflammation and structural remodeling. *Am. J. Respir. Crit. Care Med.* **169,** 378–385 (2004).
48. Andersson, C.K. *et al.* Mice lacking 12/15-lipoxygenase have attenuated airway allergic inflammation and remodeling. *Am. J. Respir. Cell. Mol. Biol.* **39,** 648–656 (2008).
49. Kapanci, Y., Ribaux, C., Chaponnier, C. & Gabbiani, G. Cytoskeletal features of alveolar myofibroblasts and pericytes in normal human and rat lung. *J. Histochem. Cytochem.* **40,** 1955–1963 (1992).
50. Xisto, D.G. *et al.* Lung parenchyma remodeling in a murine model of chronic allergic inflammation. *Am. J. Respir. Crit. Care Med.* **171,** 829–837 (2005).
51. Lundblad, L.K. *et al.* Airway hyperresponsiveness in allergically inflamed mice: the role of airway closure. *Am. J. Respir. Crit. Care Med.* **175,** 768–774 (2007).
52. Martinez, F.D. Genes, environments, development and asthma: a reappraisal. *Eur. Respir. J.* **29,** 179–184 (2007).
53. Guerra, S. & Martinez, F.D. Asthma genetics: from linear to multifactorial approaches. *Annu. Rev. Med.* **59,** 327–341 (2008).
54. Eisenbarth, S.C. *et al.* Lipopolysaccharide-enhanced, toll-like receptor 4-dependent T helper cell type 2 responses to inhaled antigen. *J. Exp. Med.* **196,** 1645–1651 (2002).
55. Fattouh, R. *et al.* Transforming growth factor-beta regulates house dust mite-induced allergic airway inflammation but not airway remodeling. *Am. J. Respir. Crit. Care Med.* **177,** 593–603 (2008).
56. Hantos, Z., Daroczy, B., Suki, B., Nagy, S. & Fredberg, J.J. Input impedance and peripheral inhomogeneity of dog lungs. *J. Appl. Physiol.* **72,** 168–178 (1992).